TITLE

Superior thermal tolerance in a wild *Oryza* species can be attributed to maintenance of Rubisco activation by a thermally stable Rubisco activase ortholog

AUTHORS

Andrew P Scafaro[1,2], Alexander Gallé[3], Jeroen van Rie[3], Elizabete Carmo-Silva[4], Michael E Salvucci[5], Brian J Atwell[1]

1. Department of Biological Sciences, Faculty of Science and Engineering, Macquarie University, Sydney, New South Wales 2109, Australia

2. ARC Centre of Excellence in Plant Energy Biology, Research School of Biology, The Australian National University, Canberra, ACT 0200, Australia

3. Bayer CropScience NV Innovation Center – Trait Research Technologiepark 38 9052 Zwijnaarde (Gent) Belgium

4. Lancaster Environment Centre, Lancaster, LA1 4YQ, UK

5. U.S. Department of Agriculture, Agricultural Research Service, Arid-Land Agricultural Research Center, Maricopa, AZ 85138, United States

AUTHOR FOR CORRESPONDENCE

Brian J Atwell

Email: brian.atwell@mq.edu.au

Phone: +61 2 9850-8224

WORD COUNT: Total (5835), Introduction (697), Materials and Methods (2169), Results (1503), Discussion (1455), Acknowledgments (11), Figures (8 - all but Fig. 5 in colour), Supporting information (1).

SUMMARY

- The response of photosynthesis and plant growth to short periods of supra-optimal heat was tested in rice (*Oryza sativa*) and two wild *Oryza* species from the Australian savanna, *O. meridionalis* and *O. australiensis*. The mechanism of heat tolerance in the wild species was explored, particularly focusing on the heat-labile protein Rubisco activase (RCA).
- We compared leaf elongation rates, net photosynthesis and Rubisco activation state at moderate (28°C) and high temperature (45°C). Sequence analysis followed by enzyme kinetics of RCA was used to identify structural differences and thermal stability.
- *Oryza australiensis* was the most heat-tolerant species. Rubisco activation state was positively correlated with leaf elongation rates across all three species at four times following exposure to 45°C. *Oryza australiensis* had multiple polymorphisms in the RCA primary protein sequence, and the protein was thermally stable up to 42°C relative to RCA from *O. sativa* which became inhibited at 36°C.
- We attribute the heat tolerance of growth and photosynthesis in these wild species to thermal stability of RCA, enabling Rubisco to remain active. Because thermal stability of RCA in *O. australiensis* co-occurs with reduced enzyme specific activity, an increased RCA to Rubisco ratio is required *in vivo* to maintain high Rubisco activation.

KEY WORDS

Heat tolerance, *Oryza australiensis*, *Oryza meridionalis*, Photosynthesis, Rice (*Oryza sativa*), Rubisco activase, Thermal stability.

INTRODUCTION

The susceptibility of photosynthesis to inhibition by moderate and high temperatures has been attributed to two major causes depending on the severity of the stress. At very high temperatures, the properties of the lipid bilayer of the thylakoid membrane change causing a disruption in the electron transports and ion transport reactions necessary for photosynthesis (Sharkey, 2005; Yamori *et al.*, 2013). At moderately high temperatures, inactivation the soluble enzyme Rubisco activase (RCA) (Crafts-Brandner & Salvucci, 2000; Salvucci *et al.*, 2001; Salvucci & Crafts-Brandner, 2004a; Sage *et al.*, 2008) affects photosynthesis by reducing the ability of RCA to maintain Rubisco in an active state. RCA is a member of the AAA+ protein family and is a regulatory partner of Ribulose-1,5-bisphosphate carboxylase/oxygenase (Rubisco). RCA keeps Rubisco in an active state through an ATP-driven remodeling of the conformation of Rubisco that effectively clears Rubisco active sites of tightly bound sugar-phosphate inhibitors (Portis, 2003; Salvucci & Crafts-Brandner, 2004a). The thermal instability of RCA has been attributed to aggregation of the protein, which is observed even at moderately high temperatures (Feller *et al.*, 1998; Rokka *et al.*, 2001; Salvucci *et al.*, 2001; Barta *et al.*, 2010).

Several studies have looked at the impact of genetically engineered RCA conformation or expression on Rubisco activity and photosynthesis under different physiological conditions (Carmo-Silva *et al.*, 2014). For example, genetically modifying Arabidopsis (*Arabidopsis thaliana*) RCA has led to improvements in its thermal stability, resulting in improved photosynthesis and growth under heat stress (Kurek *et al.*, 2007; Kumar *et al.*, 2009). Considering that RCA in species adapted to warmer climates is more thermostable than the RCA in cool-adapted species (Crafts-Brandner & Salvucci, 2000; Salvucci & Crafts-Brandner, 2004b; Carmo-Silva & Salvucci, 2011; Carmo-Silva *et al.*, 2012; Scafaro *et al.*, 2012), one promising approach is to look for genetic variation in RCA from closely related species adapted to contrasting thermal regimes. From a plant breeding perspective, genetic variation in species closely related to food crops may be a valuable source of genes for introgression into the cultivated species. Furthermore, Rubisco is functionally dependent on RCA and the two enzymes show species specificity (Wang *et al.*, 1992; Wachter *et al.*, 2013). The benefit of searching for genetic variation in closely related taxa with similar Rubisco protein structure is that RCA is more likely to be compatible. In this respect, the close relatives of *Oryza sativa* offer good opportunities in the quest for heat-tolerant photosynthesis in cultivated rice.

Of the more than 20 species in the *Oryza* genus, only two species are cultivated, *Oryza sativa* and *Oryza glaberrima* (Sweeney & McCouch, 2007) and the rest are considered 'wild' (Ge *et al.*, 1999; Vaughan *et al.*, 2008). Many of the wild species are adapted to harsh environments, as the genus is found across all tropical regions of the Earth in a vast array of climates (Atwell *et al.*, 2014) and

wild relatives harbour more than 50% of the genetic diversity found in the genus (Caicedo *et al.*, 2007; Zhu *et al.*, 2007; Xu *et al.*, 2012).

In rice, a single RCA gene encodes two isoforms through post-translational splicing of pre-mRNA into a larger (α) 45 kDa isoform and a smaller (β) 41 kDa isoform (To *et al.*, 1999). The α and β isoforms are identical except for an additional 33 amino acids at the C-terminus of the α isoforms and substitutions in the five amino acids that immediately precede this extension. Contained within this C-terminal extension is a pair of cysteine residues that can form a disulfide bond that is reduced by thioredoxin-f and is regulated by the redox state of the chloroplast (Zhang & Portis, 1999; Portis *et al.*, 2008).

Here we report on the tolerance of growth and photosynthesis to heat in five rice genotypes representing three *Oryza* species, *O. sativa* (*Os*), *O. meridionalis* (*Om*) and *O. australiensis* (*Oa*). We hypothesise that the wild relatives of rice adapted to the hot northern savanna of Australia have greater tolerance to heat. Mechanisms underpinning heat tolerance are explored and differences in the primary structure of RCA between species are implicated in thermal tolerance. Hence, we explore the heat susceptibility of RCA isoforms and identify potential mechanisms for the observed heat-stability of the enzyme.

MATERIAL AND METHODS

Plant growth

Seeds of *Oryza sativa* L. ssp. *japonica* cv. Amaroo (*Os*- A) and *O. sativa* L. ssp. *indica* cv. Doongara (*Os*-D) were obtained from the Yanco Agricultural Institute (Department Of Primary Industries, NSW, Australia). Seeds of *Oryza meridionalis* Ng. (*Om*) were collected from wild populations located in the Cape York Peninsula of Australia (*Om*-CY) at S15°42', E145°03' and from Keep River north of Western Australia (*Om*-KR) at S15°58', E129°03'. *Oryza australiensis* Domin (*Oa*) seeds were collected from the same Keep River location as *O. meridionalis*. For all experiments, plants were grown in controlled growth cabinets (Thermoline Scientific Equipment, Smithfield, NSW, Australia) under a 12-h photoperiod with a photosynthetic photon flux density (PPFD) of 600-800 μmol m^{-2} s^{-1}. Plants were grown at 28/22°C (day/night) in a 3:1, soil of fine-textured krasnozem (locally sourced from Robertson, NSW, Australia) and an organic mix in pots with no drainage holes. For leaf elongation rate experiments, plants were grown in 2-L pots and measurements were taken at the fifth-leaf stage. For all other experiments, plants were sampled after growing for 60 d in 10-L pots. Soil was kept wet at all times and allowed to pool at the surface once the plants were over 40 d

old. A commercial liquid fertiliser (AQUASOL, Yates, Australia) was applied once a week following manufacturer's instructions, beginning 10 d after germination.

Leaf elongation rates

Leaf elongation rates (LER) were measured using a HR4000 Linear Variable Displacement Transducer (LVDT) as described by Scafaro *et al*. (2010). After emergence of the fifth leaf, plants were transferred to a cabinet containing the LVDT unit and randomly assigned to one of the eight measurement stations. The fifth leaf was clipped to the apparatus and growth was measured for a 24 h period. Plants were exposed to 22°C for the initial 12 h of darkness followed by 28°C for the first 4 h of the light period. The cabinet temperature was then raised to 45°C for 4 h and returned to 28°C for the final 4 h of the day period. Leaf length was measured and logged every 6 min using the software program VuGrowth, version 1.0 (Applied Measurement, Oakleigh, Victoria, Australia). The ambient temperature of the cabinet was logged ever 10 min by a portable data logger (Onset HOBO, Massachusetts, USA) placed next to the plants. Leaf lengths were converted to LER by calculating the change in leaf length over each 1 h period. The experiment was repeated on six occasions with nine plants from each genotype measured in total.

Gas-exchange measurements

Gas-exchange was measured using a Licor 6400 (Li-Cor, Lincoln, USA). The CO_2 in the reference chamber air was set at 380 µL L^{-1} and a PPFD of 1500 µmol m^{-2} s^{-1} was used for all measurements. Measurements were made inside the growth cabinet and the air temperature of the gas exchange cuvette was set to 28 or 45°C to match cabinet temperature. Control measurements were made at 28°C beginning 2 h into the light period. Measurements at 45°C were made 4 h after the temperature was raised from 28°C, including a 30-min period of ramping before reaching 45°C. All measurements were made on healthy, fully-expanded leaves. Measurements were made on three to six leaves from three pot replicates.

DNA sequencing and sequence alignment

Total RNA was extracted from 100 mg of leaf tissue using an RNeasy Plant Mini Kit (QIAGEN, Venlo, Netherlands). RNA was converted to cDNA using a SuperScript VILO cDNA Synthesis Kit (Invitrogen, CA, USA) with 2.1 µg of RNA as a template. PCR was performed on 2 µl of the cDNA product using GoTaq Green Master Mix (Promega, Fitchberg, WI, USA). Refer to Table S1 for the

PCR cycle program and the primers used. The product was run on a 1.5% agarose gel stained with Gel Red (Biotium, Hayward, CA, USA). The bands where cut from the gel using a scalpel and the DNA purified using a DNA Gel Extraction Kit (QIAGEN, Venlo, Netherlands). The PCR products were sequenced in both directions using the same primers as PCR amplification. Sequence preparation was performed using Big Dye Terminator V3.1 sequencing reaction mix as per manufacturer's instructions and samples run on a 3130x1 Genetic Analyzer (Applied Biosystems, Foster City, CA, USA). Multiple DNA and protein sequences were aligned using the MUSCLE algorithm (Edgar, 2004) and the open-source software program Unipro UGENE v1.9.0.

Isolation of Rubisco and RCA

The α and β isoforms of Rubisco activase from *O. sativa* (RCA_{Os}) and *O. australiensis* (RCA_{Oa}) were cloned into expression vectors with or without His-Tagged C-terminals (refer to Fig. S1 for vector maps and sequences). Vectors were transformed following standard procedures into BL21(DE3) Star *Escherichia coli* for expression and purification.

All purification procedures were carried out at 4°C or below and chromatography columns and media purchased from GE Healthcare Bio-Sciences AB (Uppsala, Sweden). The method of Barta *et al*. (2011a) was used for expression and purification of RCA from *E. coli*, with some exceptions. *E. coli* cells were grown in 400-mL cultures in 1 L conical flasks and after IPTG induction (OD_{600} of 0.4-0.6) grown for a further 17 h at 25°C. Cells were lysed by passing soluble lysate through a French press at 700 bars. For non-tagged recombinant RCA, gel filtration and anion exchange chromatography was achieved using a Superose 6 10/300 GL and a 5 mL HiTrap Q HP column. Alternatively, His-trapped RCA constructs were purified using 1 mL HisTrap FF columns following manufacturer's instructions.

Rubisco activase was purified from leaves by first homogenising tissue in a mortar and pestle with liquid N_2. An extraction buffer (50 mM HEPES pH 7.2, 5 mM $MgCl_2$, 1 mM EDTA, 1 mM ATP, 10 µM leupeptin, 20 mM ascorbic acid, 50 mM 2-mercaptoethanol, 1 mM PMSF and 2% w/v PVPP) was added to homogenised tissue and vortexed for 3-5 min before being passed through cheesecloth and spun at 24,000 g for 20 min. Supernatant was collected and 35% (v/v) saturated ammonium sulphate, pH 7, added and mixed well by inversion of tubes. Samples were left on ice for 30 min before being spun at 24,000 g for 14 min. The supernatant was removed and the pellet resuspended in extraction buffer without PVPP before being desalted using Sephadex G50-fine media and desalting buffer (50 mM HEPES pH 7.2, 5 mM $MgCl_2$, 1 mM EDTA, 0.2 mM ATP, 10 µM leupeptin, 1 mM PMSF, 2 mM DTT).

The desalted sample was passed through a 2 mL Q-Sepharose anion-exchange column, followed by 5 column volumes of desalting buffer, desalting buffer + 0.2 M KCl and desalting buffer + 0.5 M KCl. The desalting buffer + 0.2 M KCl fractions containing partially purified β isoform were pooled, concentrated and stored at -80°C for use in assays. The final concentration of purified recombinant and leaf-extracted RCA was determined using Protein Assay Dye Reagent Concentrate (BIO RAD, Hercules, CA, USA) following manufacturer's instructions and compared to a BSA standard.

Rubisco was purified from leaves of *O. sativa* (Rubisco$_{Os}$) or *O. australiensis* (Rubisco$_{Oa}$) following the method of Carmo-Silva *et al*. (2011) with the following modifications. Frozen tissue was homogenised by grinding in a mortar and pestle with liquid N_2. In separate tubes, approximately 2 g of powdered tissue and 20 mL of Rubisco extraction buffer was vortexed for 3-5 min before the filtering of homogenate through cheesecloth and centrifugation. After precipitation with ammonium sulphate, 0.8 mL samples of resuspended precipitate were loaded onto sucrose gradients contained within disposable PA Ultracrimp 11.5 mL tubes (ThermoFisher Scientific, Waltham, MA, USA). Sucrose gradients were obtained by placing 0.4 M sucrose in half strength Rubisco extraction buffer and 5 mM DTT solution at -20°C overnight, followed by thawing at 4°C for another 24-h prior to use. The samples were spun at 400,000 × g for 2.5 h on a T-890 fixed angle rotor using a Sorvall WX ultracentrifuge (ThermoFisher Scientific, Waltham, MA, USA). Piercing a hole in the bottom of tubes and collecting the droplets in 1.5 mL tubes achieved fractionation. The final anion-exchange purification step was initially used but deleted from later experiments when found to be not required. Final Rubisco and RCA purity was high (Fig. S2).

Native gel and western analysis

Purified RCA stock was thawed, diluted to the desired concentration using first-stage activation buffer and 3.5 µL of NativePAGE 4 × sample buffer added to 10 µL of sample before loading onto 4-16% NativePAGE Novex Bis-Tris Gels run at 150 volts for 120 min (Invitrogen, CA, USA). NativeMark Protein Standards were used as molecular mass standards.

Prior to western analysis, extractions were completed at 4°C. Plant material was ground in liquid nitrogen and 100 mg of fine powdered tissue was weighed before being vortexed in 800 µL of soluble extraction buffer. Samples were spun at full- speed on a bench top rotor for 10-min and 10 µL of the supernatant added to 3 µL of 4 × LDS Sample Buffer (ThermoFisher Scientific, Waltham, MA, USA) containing 0.5% (v/v) 2-mercaptoethanol. Samples were run on 4-20% Mini TGX stain free gels (Bio Rad, Hercules, CA, USA) for 45-min at 200 volts. The first lane of gels was loaded with 4 µL of Precision Plus All Blue Standard (Bio Rad, Hercules, CA, USA) pre-stained molecular

mass markers. Protein was transferred to Immobilon-P PVDF membrane (Merck Millipore, Billerica, MA, USA) using a TRANS-BLOT SD Semi-Dry Transfer Cell (Bio Rad, Hercules, CA, USA) following manufacturer's instructions. Membrane was blocked with TBS (100 mM Tris, 150 mM NaCl, pH 7.5) plus 5% milk powder, washed with TBST (TBS with 0.1% (v/v) Tween 20) and stained with NBT/BCIP (Promega, Fitchberg, WI, USA). Primary polyclonal antibody was either anti-tobacco RCA (Crafts-Brandner *et al.*, 1990) or Rubisco large subunit antibody (Agrisera, Vännas, Sweden), both prepared in rabbits. Secondary antibody was goat anti-rabbit polyclonal (Sigma-Aldrich, St Louis, MO, USA). The westerns were repeated on three separate plant extractions. Image analysis of westerns was carried out using ImageJ software (National Institutes of Health, Bethesda, MA, USA) with spot area used as a determinant of abundance.

ATP hydrolysis activity

Two photometric methods were used for the determination of ATP hydrolysis (ATPase) activity. The first was a coupled reaction in which NADH was reduced to NAD^+ in equal proportion to ADP production and subsequent measurement of reduction in absorbance at 340 nm (Barta *et al.*, 2011b). The extinction coefficient of NADH, 6.22 mM cm^{-1} was used to calculate activity in Units (U), which equates to 1 µmol of ATP hydrolysed per min. Samples were run in 96-well plates with 10 µg of RCA added to a final 150 µL volume reaction mix. The second method measured P_i liberated from ATP during hydrolysis through absorbance at 850 nm (Chifflet *et al.*, 1988). Potassium phosphate at concentrations of 50 to 400 µM was used as a standard. 20 µg of RCA was added to a final 50 µL reaction and run for 20 min before inhibition with 12% SDS. Reactions were run in 1.5 mL tubes and incubated at set temperatures using a tube heating apparatus (Eppendorf, Hamburg, Germany). The P_i method was used for temperature- dependent experiments as it enabled more accurate control of temperature than the NADH coupled assay. All photometric measurements were made on a Pherastar FS plate reader (BMG Labtech Pty. Ltd. Ortenberg, Germany).

Activation of Rubisco by RCA

The activation of Rubisco by RCA was determined using the two-stage method of Barta *et al.* (2011b) with the following exceptions. In the first-stage reaction buffer, 6 mM rather than 4 mM RuBP was used. In all cases 1.5 mg mL^{-1} Rubisco was used in the first-stage reaction, the reaction was run for 5 min at given temperatures before transfer of 50 µL to the second-stage reaction which was run for 30 sec at 30°C before quenching. The quenched samples were transferred to 20 mL

glass scintillation vials, dried on a heating block set to 80°C and resuspended in 200 µL of 0.1 M HCl. 5 mL of Biodegradable Counting Scintillant (GE Healthcare Bio- Sciences AB, Uppsala, Sweden) was added, mixed and disintegrations per minute were measured on a Tri-Carb 2910 TR Liquid Scintillation Analyzer (PerkinElmer, Waltham, MA, USA). All activation results are given as the fraction of Rubisco sites re-activated by RCA over the 5-min incubation period (fraction activated). Rubisco re-activated in the absence of RCA was subtracted.

To determine the activation state of Rubisco, two 0.266 cm^2 leaf disks were rapidly excised from mature fully expanded leaves using a leaf punch and immediately frozen in liquid nitrogen. The Rubisco activation state was calculated by measuring total and initial Rubisco activities. Samples were collected throughout the light period to coincide with growth measurements. Samples were collected after 2 h at 28°C, 2 h at 45°C, 4 h at 45°C and 1 h after temperature was returned to 28°C. Four replicates were collected from separate pots placed randomly throughout the cabinet.

Statistics

All graphs and statistics were created using GraphPad Prism 5.0d software (GraphPad Prism Software Inc., San Diego, USA). Differences between species in Rubisco, RCA and gas-exchange values were analysed with a two-tailed t-test.

RESULTS

Temperature-dependent growth and photosynthesis of *Oryza* genotype

The heat sensitivity of growth and photosynthesis differed among the three *Oryza* species. The instantaneous hourly response to increased day temperature was observed by analysis of leaf elongation rates (LER) (Fig. 1). At the end of the dark period, all genotypes had a similar LER about 2 mm h^{-1}. At the commencement of the light period when temperature increased from 22°C to 28°C, LER increased to between 3-4 mm h^{-1} for all genotypes except *Om*-CY, where LER did not exceed 3 mm h^{-1}. When the plants were heat-shocked, with day air-temperature raised from 28 to 45°C over a period of approximately 30 min, LERs were stable or increased during the first hour before declining (*Os*, *Om*) or remaining stable (*Oa*) over the next 3 h at 45°C, indicating species-specific differences in the response to high temperature. Relative to *Os*- A, the LER after 4 h at 45°C was higher for all genotypes. *Os*- D, a long-grained cultivar of *Os*, was more heat tolerant than the japonica cultivar *Os*-A but less tolerant than either of the wild relatives of rice. The two *Om*

accessions had a similar response and their heat tolerance was intermediate between *Os* and *Oa*. *Oa* showed the greatest tolerance to high temperature and after 4 h of exposure to 45°C the LER of *Oa* was double that of *Os*-A and significantly higher than all of the other genotypes.

The significant role of photosynthesis for growth and thermal tolerance of rice was established by measuring leaf gas-exchange at the ambient and elevated temperatures (Fig. 2). Like LER, the effect of elevated temperature on net photosynthetic rate (P_n) was also species-specific. After 4 h at 45°C, net photosynthesis significantly decreased for all the genotypes, except *Oa*. The decrease in P_n was more marked for *Os* (42% for *Os*-A and 39% for *Os*-D) and intermediate for *Om* (25% for *Om*-CY and 29% for *Om*-KR). Inhibition of P_n was not caused by lower stomatal conductance (g_s) since g_s did not significantly change for *Os*-A or *Om* genotypes and actually increased for *Oa* at 45°C (Fig. 2b). Sustained g_s during exposure to 45°C resulted in significantly high rates of transpiration and subsequent leaf cooling of 3.2 to 6.3°C below ambient air temperature across all genotypes (Fig. 2 c,d). *Oa*, the only species to have a significant increase in g_s at 45°C, had the lowest leaf temperature during heat treatment.

The activation state of Rubisco was measured and its response to heat was correlated with LER across the five genotypes (Fig. 3). As with P_n, activation state declined to the greatest extent during heat in the two *Os* cultivars, with *Om* accessions exhibiting an intermediate decline and *Oa* showing no impairment in activation compared with control plants after 4 h of heat exposure. The consistent genotypic contrasts observed in Figs 1 a,b are reflected in the scatterplot of the mean values of Rubisco activation state versus LER for the various genotypes and temperatures (Fig. 3b). The significant positive linear relationship ($P<0.01$, $R^2=0.53$) between LER and Rubisco activation state suggested that plants maintaining Rubisco in an active state also grew the fastest.

Sequencing of the RCA gene and protein alignment

Primers designed against RCA-specific mRNA from *Os* matched *Om* and *Oa* RCA sequence and enabled sequencing of RCA α and β isoform mRNA extracted from leaves of all genotypes. Alignment of the corresponding DNA sequence showed differences in gene sequence between each of the three species (Fig. 4). There were no SNPs between the two *Om* accessions analysed so sequence divergence separated species but did not distinguish populations. Of the 1302 translated nucleotides of the β isoform, there were six SNPs between *Os* and *Om* and no difference in the α C-terminal extension. There were 49 SNPs between *Os* and *Oa*, including six deletions and a SNP unique to either the α or β isoform. There were three fewer SNPs when *Om* was compared with *Oa* rather than *Os*.

Translation of the DNA sequence revealed differences in the RCA primary sequence between

species (Fig. 4b). Interestingly, although there were 6 SNPs between *Os* and *Om*, none translated to differences at the protein level. In contrast, the genetic diversity between *Os* and *Oa* RCA led to 17 residue changes in the primary sequence between the species, including two residue deletions and a substitution unique to the C- terminal of both the α and β isoform of *Oa*. Differences in the primary structure between *Os* and *Oa* were biased towards either the N-terminal or C-terminal regions of the protein.

***In vivo* Rubisco and RCA content**

Quantitation of Rubisco and RCA by immunoblotting analyses of leaf extracts was used to estimate the *in vivo* concentration of RCA and Rubisco in *Os*-A and *Oa* leaves (Fig. 5). Given that the activity of RCA is coupled to Rubisco, the ratio of the two enzymes will affect activation activity. Importantly, while there was no significant difference in concentrations of Rubisco (P=0.36, T=0.9975, DF=5) between the two species, *Oa* had four times more RCA than *Os* on a fresh weight basis (P=0.009, T=3.84, DF=6).

Temperature-dependent Rubisco activation by leaf-extracted RCA

RCA β isoforms from *Os* (RCA*Os*) and *Oa* (RCA*Oa*) leaves were purified by ammonium sulphate precipitation in conjunction with anion-exchange chromatography. Purity reached 70% based on image analysis of the final protein extract run on SDS-PAGE (Fig. S3). The α isoform eluted in a higher salt fraction but was contaminated with high Rubisco content and was excluded from analysis.

The temperature stability of RCA*Oa* was far greater than that of RCA*Os* (Fig. 6). The activation of Rubisco by RCA*Oa* was not inhibited over the temperature range tested, including at the highest measured temperature of 42°C. By comparison, RCA*Os* became inhibited at temperatures above 34°C. The specific activity of RCA was substantially greater for RCA*Os* than RCA*Oa*. By increasing the concentration of RCA*Oa* relative to Rubisco in the assay, the activation of Rubisco became comparable to that achieved by RCA*Os*, while still maintaining superior thermal tolerance (Fig. 6).

Recombinant RCA activity

To further elucidate differences in RCA between *Os* and *Oa*, the gene from each species was expressed recombinantly and the concentration- and temperature- dependent ATP hydrolysis and activation activity of the proteins studied.

When examined in response to RCA concentration, there was a clear sigmoidal relationship between RCA concentration and the activation of Rubisco for both the α and β isoforms of each species (Fig. 7 a,b). Allosteric sigmoidal curves were fitted to each data set and the goodness-of-fit found to be high (R^2 > 0.9). Purified recombinant *Os* and *Oa* RCA were electrophoresed on native gels to estimate the molecular mass of the RCA self-oligomer and to determine whether the concentration of subunits had an impact on oligomer formation and activity. Protein concentration had a strong impact on the oligomer complex size of both species and isoforms, with a general shift from smaller (dimers) to larger (pentamers, hexamers and heptamers) complexes with increasing concentrations that corresponded to maximum RCA activity. At low RCA concentrations, the α isoform was less active than the β isoform. However, with an increase in RCA concentration, difference in the Rubisco activation between the two isoforms diminished until it was eliminated at the highest RCA concentrations measured. The fraction of Rubisco sites activated by RCA never exceeded 0.6 for either species, even after increasing the RCA to Rubisco ratio. That is, with a concentration of 1.5 mg mL^{-1} of uncarbamylated Rubisco and in presence of 6 mM RuBP, a seemingly infinite amount of RCA could only reactivate a maximum of 60% of Rubisco sites.

The relationship between RCA concentration and its ATP hydrolysis activity was also measured for the two species (Fig. 7 c,d). The specific activity of both isoforms increased substantially with increasing RCA concentration, in a similar allosteric sigmoidal manner to that of Rubisco activation. At low RCA concentrations, ATP hydrolysis activity of the α isoform was less than the β isoform, consistent with the lower specific activity of activation by the α isoform.

The temperature-dependent ATPase and Rubisco activation activity of recombinant RCA was measured (Fig. 8). Similar to findings in the leaf extracts, RCA$_{Os}$ β had markedly greater ATPase and activation specific activity than that of the corresponding RCA$_{Oa}$ isoform, but only when RCA was paired with Rubisco extracted from *Os*. When RCA was paired with Rubisco extracted from *Oa*, the specific activity of the RCA$_{Oa}$ β isoform was greater than that of RCA$_{Os}$ β. The α isoform had similar specific activity when paired with Rubisco from *Oa* but had less activity than RCA$_{Os}$ α when paired with Rubisco from *Os*. Significantly, unlike the leaf-extracted RCA, there was no observable difference in thermal stability between *Os* and *Oa* recombinant RCA, with inhibition occurring between 34 to 38°C for both species and isoforms. Furthermore there was no difference in temperature-dependent ATPase activity between the species, and the specific activity of ATP hydrolysis did not decline until temperature exceeded 36-40°C, higher than the temperature at which Rubisco activation was inhibited.

DISCUSSION

Differences in thermal tolerance between rice genotypes

Five rice genotypes, representing two cultivars of domesticated rice (*Oryza sativa*) and three accessions of two wild rice species (*O. meridionalis* and *O. australiensis*), showed different levels of tolerance to high day temperatures, consistent with the climatic characteristics of their natural range. Similarly, a previous report showed that among cultivated rice genotypes, *Os*-A is more cold tolerant/heat sensitive than *Os*-D (Jacobs & Pearson, 1999). Based on the temperature regimes at which *Om* and *Oa* populations have evolved (Atwell *et al.*, 2014) we expected the Australian wild relatives should have greater tolerance to heat than cultivated rice from south-east Asia and we found this to be true. The response to elevated temperature was most similar *within* each species, regardless of its geographic origin, indicating that differences in growth and photosynthetic rates under high temperature regimes was determined by evolutionary divergence of the wild rice species. Specifically, the identical RCA*Oa* sequence in plants collected from the most remote boundaries of the natural range of *Oa* makes localised evolutionary divergence in heat tolerance seem less likely. Notwithstanding, Juliano *et al*. (2005) have shown that *O. meridionalis* is undergoing speciation as a result of limited gene transfer between isolated populations. Thus, a broader analysis of *O. meridionalis* and other wild species is needed to determine whether there is a link between habitat and genotypic divergence in heat tolerance.

The temperature-dependent stability of leaf-extracted RCA

The positive linear correlation between Rubisco activation state and LER across all three *Oryza* species and sampling times implies that Rubisco activity is a factor determining growth rates, with low Rubisco activity impairing photosynthesis under high temperatures in rice. Knowing that RCA is responsible for activating sites on Rubisco, we conducted a deeper analysis of RCA. Critically, RCA*Oa* had substantially greater thermal stability than RCA*Os* (Fig. 6), which may explain the heat stability of Rubisco activation, photosynthesis and growth in *Oa*. Although RCA*Oa* had superior thermal stability, it supported much lower rates of Rubisco activation than RCA*Os* across the entire temperature range. Proteolysis of RCA*Oa* prior to assays cannot be excluded. Alternatively, the reduced level of activation by RCA*Oa* supports a recent postulate (Parry *et al.*, 2013) that increased thermal stability of RCA would be associated with a reduction in activating potential at moderate temperature due to restraints on conformational flexibility of RCA. Furthering this argument, almost all of the divergence in RCA between *Os* and *Oa* occurred in the terminal domains of the protein. Current information

on the crystal structure of the RCA holoenzyme indicates N and C terminal domains are inherently unstable and flexible (Stotz *et al.*, 2011) and these terminal domains are thought to be crucial for Rubisco recognition and binding (Li *et al.*, 2005; Stotz *et al.*, 2011). We postulate that changes in RCA*Oa* structure relative to RCA*Os* resulted in reduced flexibility in the terminal domains, improving thermal stability of activation, at a cost of decreased specific activity. This hypothesis is supported by the general view that reduced flexibility in proteins is the major avenue through which thermal stability can be improved (Závodszky *et al.*, 1998). Increasing the ratio of RCA*Oa* to Rubisco enhanced *in vitro* Rubisco activation (Fig. 6). When seen in the light of *Oa* having significantly higher *in vivo* concentrations of RCA, the reduced specific activity of RCA*Oa* seems to have been compensated by greater RCA content in leaves.

The concentration and temperature-dependent activity of recombinant RCA

ATPase and Rubisco activation activity of RCA in conjunction with native gels demonstrates that rice RCA must form a complex greater than a dimer to reach optimal functionality (Fig. 7). It is known that RCA forms a homo- oligomeric complex and this complex is dependent on the concentration of the enzyme, with higher concentrations leading to larger complexes (Salvucci, 1992; Wang *et al.*, 1993; Barta *et al.*, 2010; Chakraborty *et al.*, 2012; Keown *et al.*, 2013). The activity of RCA, in terms of ATP hydrolysis specific activity, was reduced at low RCA concentrations. Reduced ATPase specific activity of RCA at low concentrations also occurs in spinach (Wang *et al.*, 1993; Lilley & Portis Jr, 1997) and tobacco (Keown *et al.*, 2013). However, further to these previous observations, we show that Rubisco activation was impaired when RCA was present at low concentrations. The sigmoidal response in RCA concentration- dependent activation demonstrates that, in rice, the ability of RCA to activate Rubisco is dependent on the formation of self- assembled complexes. The dicot species tobacco (*Nicotiana tabacum* L.), spinach (*Spinacia oleracea* L.) and Arabidopsis have a linear, as opposed to sigmoidal, activation response to RCA concentration (Robinson *et al.*, 1988; Salvucci, 1992; Lilley & Portis Jr, 1997; Carmo-Silva & Salvucci, 2011). The concentration-dependent sigmoidal response of Rubisco activation which we now report in rice suggests that the strength of the interaction of RCA monomers must be species dependent, where a sufficiently high RCA concentration is particularly critical for formation of complexes and subsequent Rubisco activation in rice. This finding supports a previous study of Rubisco activation by leaf-extracted RCA, in which rice was shown to have minimal detectable RCA activity relative to other species, including tobacco, postulated to be related to differences in self-association of RCA (Carmo-Silva & Salvucci, 2011).

Because a difference was found between the thermal stability of Rubisco activation for the recombinant and leaf- extracted forms of RCA*Oa* (Fig. 6 and Fig. 8), other factor(s) must be involved in thermal stability of RCA*Oa in vivo*. This could be explained by protein-protein interactions or an *in vivo* post-translational modification of RCA*Oa*, however the mechanism remains unexplained.

For both recombinant RCA*Os* and RCA*Oa*, ATPase specific activity was inhibited at >36°C (Fig. 8) while Rubisco activation by RCA began to decline steadily at temperatures above 30°C. Previous reports show a general trend that ATPase activity reflects activation activity (Robinson & Portis Jr, 1989; Salvucci & Crafts-Brandner, 2004b). The difference in thermal stability between the ATP hydrolysis and Rubisco activation by rice RCA suggests that inhibition is not entirely due to thermal instability and insoluble aggregation of the RCA protein alone (i.e. as reflected by RCA-dependent ATPase activity), but more subtly due to thermal instability of the interaction between Rubisco and RCA (i.e. the activation of Rubisco).

For both species recombinant α isoform had lower ATPase and activation activity than the β isoform across the measured temperature range at the molar ratio of RCA to Rubisco measured. It is known that two conserved cysteine residues in the α isoform C-terminal extension form a disulphide bond that reduces ATPase and activation activity, and that reduction of this bond increases activity and requires thioredoxin-f (Zhang & Portis, 1999). The addition of thioredoxin-f in assays could have substantially increased activity of the α isoform, however this was not tested. Although we found the α isoform to be slightly more thermostable at 34°C, the subtle difference in thermal stability between the isoforms is interesting considering reports showing α rather than β mRNA to be upregulated and protein abundance to increase with heat in rice (Scafaro *et al.*, 2010; Wang *et al.*, 2010) and the α isoform to have greater ATPase thermal stability than the β isoform in spinach (Crafts-Brandner *et al.*, 1997; Keown & Pearce, 2014). We speculate that increased α to β isoform ratio in rice RCA with heat may be a mechanism to regulate the Calvin cycle in response to redox changes related to photosystem damage, rather than purely a mechanism to increase RCA activity at high temperature. The hypothesis that redox regulation of the α isoform C-terminal cysteine residues may change the heat stability of the enzyme should be explored.

Finally, activation of Rubisco by RCA varied depending on the isoform and origin of the Rubisco with which it was interacting. This contrast occurred despite the Rubisco large subunit of *Os* and *Oa* only having four different amino acids (Fig. S4). However, it could be critical that one of the four *Oa* substitutions is D94E. When Asp is substituted with Lys at the same position in *Chlamydomonas*, it resulted in significant changes to spinach and tobacco RCA specificity for *Chlamydomonas* Rubisco (Ott *et al.*, 2000).

Conclusions

The variation in heat susceptibility of growth among the three *Oryza* species studied was related to the level of photosynthetic inhibition at elevated temperature, which in turn correlated with the degree to which Rubisco was deactivated. In all three of these aspects, the species *Oa* had by far greater heat tolerance and we attribute this to modifications in its C and N terminal primary protein structure of RCA. The divergence in protein structure stabilised its interaction with Rubisco at high temperature. However, thermal stability came at a cost at the bio chemical level, reducing RCA specific activity at optimal temperatures. This may have been compensated for by higher RCA to Rubisco ratios for *Oa in vivo*.

ACKNOWLEDGMENTS

We would like to thank Dr Artur Sawicki for laboratory guidance.

REFERENCES

Atwell BJ, Wang H, Scafaro AP. 2014. Could abiotic stress tolerance in wild relatives of rice be used to improve *Oryza sativa*? *Plant Science* **215–216**: 48-58.

Barta C, Carmo-Silva AE, Salvucci ME. 2011a. Purification of rubisco activase from leaves or after expression in *Escherichia coli*. *Methods in Molecular Biology* **684**: 363-374.

Barta C, Carmo-Silva AE, Salvucci ME. 2011b. Rubisco activase activity assays. *Methods in Molecular Biology* **684**: 375-382.

Barta C, Dunkle AM, Wachter RM, Salvucci ME. 2010. Structural changes associated with the acute thermal instability of rubisco activase. *Archives of Biochemistry and Biophysics* **499**: 17-25.

Caicedo AL, Williamson SH, Hernandez RD, Boyko A, Fledel-Alon A, York TL, Polato NR, Olsen KM, Nielsen R, McCouch SR, Bustamante CD, Purugganan MD. 2007. Genome-wide patterns of nucleotide polymorphism in domesticated rice. *PLoS Genetics* **3**: e163.

Carmo-Silva E, Barta C, Salvucci ME. 2011. Isolation of ribulose-1,5-bisphosphate carboxylase/oxygenase from leaves. *Methods in Molecular Biology* **684**: 339-347.

Carmo-Silva E, Gore MA, Andrade-Sanchez P, French AN, Hunsaker DJ, Salvucci ME. 2012. Decreased CO_2 availability and inactivation of rubisco limit photosynthesis in cotton plants under heat and drought stress in the field. *Environmental and Experimental Botany* **83**: 1-11.

Carmo-Silva E, Salvucci M. 2011. The activity of rubisco's molecular chaperone, rubisco activase, in leaf extracts. *Photosynthesis Research* **108**: 143-155.

Carmo-Silva E, Scales JC, Madgwick PJ, Parry MAJ. 2014. Optimizing rubisco and its regulation

for greater resource use efficiency. *Plant, Cell & Environment*: doi: 10.1111/pce.12425.

Chakraborty M, Kuriata AM, Nathan Henderson J, Salvucci ME, Wachter RM, Levitus M. 2012. Protein oligomerization monitored by fluorescence fluctuation spectroscopy: Self-assembly of rubisco activase. *Biophysical Journal* **103**: 949-958.

Chifflet S, Torriglia A, Chiesa R, Tolosa S. 1988. A method for the determination of inorganic phosphate in the presence of labile organic phosphate and high concentrations of protein: Application to lens ATPases. *Analytical Biochemistry* **168**: 1-4.

Crafts-Brandner SJ, Salvucci ME. 2000. Rubisco activase constrains the photosynthetic potential of leaves at high temperature and CO2. *Proceedings of the National Academy of Sciences of the United States of America* **97**: 13430-13435.

Crafts-Brandner SJ, Salvucci ME, Egli DB. 1990. Changes in ribulose bisphosphate carboxylase/oxygenase and ribulose 5-phosphate kinase abundances and photosynthetic capacity during leaf senescence. *Photosynthesis Research* **23**: 223-230.

Crafts-Brandner SJ, van de Loo FJ, Salvucci ME. 1997. The two forms of ribulose-1,5-bisphosphate carboxylase/oxygenase activase differ in sensitivity to elevated temperature. *Plant Physiology* **114**: 439-444.

Edgar RC. 2004. Muscle: Multiple sequence alignment with high accuracy and high throughput. *Nucleic Acids Research* **32**: 1792-1797.

Feller U, Crafts-Brandner SJ, Salvucci ME. 1998. Moderately high temperatures inhibit ribulose-1,5- bisphosphate carboxylase/oxygenase (rubisco) activase- mediated activation of rubisco. *Plant Physiology* **116**: 539-546.

Ge S, Sang T, Lu B-R, Hong D-Y. 1999. Phylogeny of rice genomes with emphasis on origins of allotetraploid species. *Proceedings of the National Academy of Sciences of the United States of America* **96**: 14400- 14405.

Jacobs BC, Pearson CJ. 1999. Growth, development and yield of rice in response to cold temperature. *Journal of Agronomy & Crop Science* **182**: 79-88.

Juliano AB, Naredo ME, Lu B-R, Lu, Jackson M, T 2005. Genetic differentiation in *Oryza meridionalis* Ng based on molecular and crossability analyses. *Genetic Resources and Crop Evolution* **V52**: 435-445.

Keown JR, Griffin MDW, Mertens HDT, Pearce FG. 2013. Small oligomers of ribulose-bisphosphate carboxylase/oxygenase (rubisco) activase are required for biological activity. *Journal of Biological Chemistry* **288**: 20607-20615.

Keown JR, Pearce FG. 2014. Characterization of spinach ribulose-1,5-bisphosphate

carboxylase/oxygenase activase isoforms reveals hexameric assemblies with increased thermal stability. *Biochemical Journal* **464**: 413-423.

Kumar A, Li C, Portis A. 2009. *Arabidopsis thaliana* expressing a thermostable chimeric rubisco activase exhibits enhanced growth and higher rates of photosynthesis at moderately high temperatures. *Photosynthesis Research* **100**: 143-153.

Kurek I, Chang TK, Bertain SM, Madrigal A, Liu L, Lassner MW, Zhu G. 2007. Enhanced thermostability of Arabidopsis rubisco activase improves photosynthesis and growth rates under moderate heat stress. *Plant Cell* **19**: 3230-3241.

Li C, Salvucci ME, Portis AR. 2005. Two residues of rubisco activase involved in recognition of the rubisco substrate. *Journal of Biological Chemistry* **280**: 24864- 24869.

Lilley RM, Portis Jr AR. 1997. ATP hydrolysis activity and polymerization state of ribulose-1,5-bisphosphate carboxylase oxygenase activase (do the effects of Mg^{2+}, K^{+}, and activase concentrations indicate a functional similarity to actin?). *Plant Physiology* **114**: 605-613.

Ott CM, Smith BD, Portis AR, Spreitzer RJ. 2000. Activase region on chloroplast ribulose-1,5-bisphosphate carboxylase/oxygenase: Nonconservative substitution in the large subunit alters species specificity of protein interaction. *Journal of Biological Chemistry* **275**: 26241-26244.

Parry MAJ, Andralojc PJ, Scales JC, Salvucci ME, Carmo- Silva AE, Alonso H, Whitney SM. 2013. Rubisco activity and regulation as targets for crop improvement. *Journal of Experimental Botany* **64**: 717-730.

Portis A. 2003. Rubisco activase – rubisco's catalytic chaperone. *Photosynthesis Research* **75**: 11-27.

Portis AR, Li C, Wang D, Salvucci ME. 2008. Regulation of rubisco activase and its interaction with rubisco. *Journal of Experimental Botany* **59**: 1597-1604.

Robinson SP, Portis Jr AR. 1989. Adenosine triphosphate hydrolysis by purified rubisco activase. *Archives of Biochemistry and Biophysics* **268**: 93-99.

Robinson SP, Streusand VJ, Chatfield JM, Portis AR. 1988. Purification and assay of rubisco activase from leaves. *Plant Physiology* **88**: 1008-1014.

Rokka A, Zhang L, Aro E-M. 2001. Rubisco activase: An enzyme with a temperature-dependent dual function? *The Plant Journal* **25**: 463-471.

Sage RF, Way DA, Kubien DS. 2008. Rubisco, rubisco activase, and global climate change. *Journal of Experimental Botany* **59**: 1581-1595.

Salvucci ME. 1992. Subunit interactions of rubisco activase: Polyethylene glycol promotes self-association, stimulates ATPase and activation activities, and enhances interactions with rubisco. *Archives of Biochemistry and Biophysics* **298**: 688-696.

Salvucci ME, Crafts-Brandner SJ. 2004a. Inhibition of photosynthesis by heat stress: The activation state of rubisco as a limiting factor in photosynthesis. *Physiologia Plantarum* **120**: 179-186.

Salvucci ME, Crafts-Brandner SJ. 2004b. Relationship between the heat tolerance of photosynthesis and the thermal stability of rubisco activase in plants from contrasting thermal environments. *Plant Physiology* **134**: 1460-1470.

Salvucci ME, Osteryoung KW, Crafts-Brandner SJ, Vierling E. 2001. Exceptional sensitivity of rubisco activase to thermal denaturation *in vitro* and *in vivo*. *Plant Physiology* **127**: 1053-1064.

Scafaro AP, Haynes PA, Atwell BJ. 2010. Physiological and molecular changes in *Oryza meridionalis* Ng., a heat- tolerant species of wild rice. *Journal of Experimental Botany* **61**: 191-202.

Scafaro AP, Yamori W, Carmo-Silva AE, Salvucci ME, von Caemmerer S, Atwell BJ. 2012. Rubisco activity is associated with photosynthetic thermotolerance in a wild rice (*Oryza meridionalis*). *Physiologia Plantarum* **146**: 99-109.

Sharkey TD. 2005. Effects of moderate heat stress on photosynthesis: Importance of thylakoid reactions, rubisco deactivation, reactive oxygen species, and thermotolerance provided by isoprene. *Plant, Cell & Environment* **28**: 269-277.

Stotz M, Mueller-Cajar O, Ciniawsky S, Wendler P, Hartl FU, Bracher A, Hayer-Hartl M. 2011. Structure of green-type rubisco activase from tobacco. *Nature Structural & Molecular Biology* **18**: 1366-1370.

Sweeney M, McCouch S. 2007. The complex history of the domestication of rice. *Annals of Botany* **100**: 951-957.

To K-Y, Suen D-F, Chen S-CG. 1999. Molecular characterization of ribulose-1,5-bisphosphate carboxylase/oxygenase activase in rice leaves. *Planta* **209**: 66-76.

Vaughan DA, Lu B-R, Tomooka N. 2008. The evolving story of rice evolution. *Plant Science* **174**: 394-408.

Wachter R, Salvucci M, Carmo-Silva AE, Barta C, Genkov T, Spreitzer R. 2013. Activation of interspecies-hybrid rubisco enzymes to assess different models for the rubisco–rubisco activase interaction. *Photosynthesis Research* **117**: 557-566.

Wang D, Li XF, Zhou ZJ, Feng XP, Yang WJ, Jiang DA. 2010. Two rubisco activase isoforms may play different roles in photosynthetic heat acclimation in the rice plant. *Physiologia Plantarum* **139**: 55-67.

Wang Z-Y, Snyder GW, Esau BD, Portis AR, Ogren WL. 1992. Species-dependent variation in the interaction of substrate-bound ribulose-1,5-bisphosphate carboxylase/oxygenase (rubisco)

and rubisco activase. *Plant Physiology* **100**: 1858-1862.

Wang ZY, Ramage RT, Portis Jr AR. 1993. Mg^{2+} and ATP or adenosine 5′-[γ-thio]-triphosphate (ATPγs) enhances intrinsic fluorescence and induces aggregation which increases the activity of spinach rubisco activase. *Biochimica et Biophysica Acta (BBA) - Protein Structure and Molecular Enzymology* **1202**: 47-55.

Xu X, Liu X, Ge S, Jensen JD, Hu F, Li X, Dong Y, Gutenkunst RN, Fang L, Huang L, Li J, He W, Zhang G, Zheng X, Zhang F, Li Y, Yu C, Kristiansen K, Zhang X, Wang J, Wright M, McCouch S, Nielsen R, Wang J, Wang W. 2012. Resequencing 50 accessions of cultivated and wild rice yields markers for identifying agronomically important genes. *Nature Biotechnology* 30: 105-111.

Yamori W, Hikosaka K, Way D. 2013. Temperature response of photosynthesis in C3, C4, and CAM plants: Temperature acclimation and temperature adaptation. *Photosynthesis Research*: 1-17.

Závodszky P, Kardos J, Svingor Á, Petsko GA. 1998. Adjustment of conformational flexibility is a key event in the thermal adaptation of proteins. *Proceedings of the National Academy of Sciences* **95**: 7406-7411.

Zhang N, Portis AR. 1999. Mechanism of light regulation of rubisco: A specific role for the larger rubisco activase isoform involving reductive activation by thioredoxin-f. *Proceedings of the National Academy of Sciences* **96**: 9438-9443.

Zhu Q, Zheng X, Luo J, Gaut BS, Ge S. 2007. Multilocus analysis of nucleotide variation of *Oryza sativa* and its wild relatives: Severe bottleneck during domestication of rice. *Molecular Biology and Evolution* **24**: 875-888.

SUPPORTING INFORMATION

Table S1. PCR cycle and primers used for the sequencing of RCA.

Fig. S1. Plasmid maps and sequences used for recombinant RCA generation.

Fig. S2. SDS-PAGE demonstrating the purity of isolated Rubisco and RCA used in enzyme kinetics.

Fig. S3. SDS-PAGE and image analysis determining leaf extracted RCA purity.

Fig. S4. Protein sequence alignment of the Rubisco large subunit from *O. sativa* and *O. australiensis*.

FIGURE LEGENDS

Figure 1. The effect of heat on leaf elongation rate (LER) during a 12-h light period, for cultivated *Oryza sativa* cv. Amaroo (*Os*-A) and Doongara (*Os*-D) (a) and wild *Oryza* genotypes, *O. meridionalis* accessions Cape York (*Om*-CY) and Keep River (*Om*-KR) (b) and *O. australiensis* (*Oa*) (c). The average values of the two cultivars of *O. sativa* and two accessions of *O. meridionalis* were compared to *O. australiensis* (d). The solid black line indicates the air temperature of the growth cabinet (right y-axes). Values are means ± SE of six experimental and nine pot replicates.

Figure 2. The effect of 28°C and 4 h at 45°C on net photosynthesis (P_n), stomatal conductance (g_s), transpiration (E) and the difference between leaf and air temperature (T_{leaf}-T_{air}) for each genotype, as described in Fig. 1. Differences between the temperature treatments were determined using a two-tailed t-test and * indicates significance at $P < 0.05$, ** significance at $P < 0.01$ and *** significance at $P < 0.001$. Values are means ± SE of three pot replicates.

Figure 3. The effect of 28°C, 2 and 4 h at 45°C and 1 h recovery (28°C) on Rubisco activation state for the five genotypes (a). Values are means ± SE of four pot replicates. (b) The mean Rubisco activation state for each genotype at each growth treatment was plotted against the mean LER at the corresponding time point (time points 2, 6, 8 and 9-h of Fig. 1) and a linear regression analysis was performed (Rubisco activation state=15.85LER+2.025, P=0.0003, R^2=0.53). Symbols and colours are the same as Fig. 1.

Figure 4. (A) DNA sequence alignment of the coding region of RCA from *O. sativa* cv. Nipponbare and cv. Amaroo (α, BAC78572.1; β, BAA97584.1), *O. meridionalis* C.Y and K.R (α, KR871000; β, KR871001) and *O. australiensis* (α, KR871002; β, KR871003). Filled squares represent nucleotide differences between *O. sativa* and *O. meridionalis* (blue), between *O. sativa* and *O. australiensis* (red) and between *O. sativa* and both *O. meridionalis* and *O. australiensis* (orange). (B) Protein alignment of the nucleotide sequence given in panel A. Note that the only difference between the two isoforms is a divergence of 38 residues at the carboxyl terminal of the proteins. The asterisk denotes the five C-terminal amino acids of the β isoform. The red-filled squares are differences in residues between the protein sequences. The colour-coded shaded areas depict functional domains of the protein, determined by crystal structure analysis of tobacco RCA (Stotz *et al*., 2011) and adapted to the rice sequence through identification of sequence homology.

Figure 5. Representative western blots of Rubisco (a) and RCA (b) to establish the amount of protein in mature leaf tissue of each species. Protein was extracted from the leaf of *Os*-A or *Oa* and run against known quantities of purified Rubisco or RCA as indicated.

Figure 6. The temperature-dependent fraction of Rubisco sites activated by RCA β isoform purified from leaves of *O. sativa* or *O. australiensis*. Rates are presented as that obtained with 0.24 mg mL^{-1} of leaf-RCA*Os* β, or the rates at three concentrations (0.24, 0.49 or 0.96 mg mL^{-1}) of RCA*Oa* β, as indicated. In all assays 1.5 mg mL^{-1} of Rubisco was used. Symbols and colours are the same as Fig. 1. Values are means ± standard error of four experimental replicates.

Figure 7. The concentration-dependent activation (a, b) and ATPase activity (c, d) of recombinant α and β isoforms of *O. sativa* and *O. australiensis* RCA. Native gel electrophoresis of RCA α and β isoforms, with the concentration of RCA loaded per lane varying from 0.01 to 0.6 mg mL^{-1}, are aligned above the corresponding concentration on the graphs. For the fraction of Rubisco sites activated by RCA, a concentration of 1.5 mg mL^{-1} of Rubisco was used in all assays. Allosteric sigmoidal curves were fitted to all data sets. Error bars are the means ± standard error of four experimental replicates.

Figure 8. Temperature-dependent ATP hydrolysis (a, b), fraction of Rubisco*Os* (c, d) and activation of Rubisco*Oa* (e, f) activated (FA) by recombinant RCA*Os* and RCA*Oa* α and β isoforms. Values relative to obtained at 30°C are provided (b, d, f). For both *O. sativa* and *O. australiensis* 0.24 mg mL^{-1} of RCA was added to a concentration of 1.5 mg mL^{-1} of Rubisco.
Symbols are the same as Fig. 7 and values are the means ± standard error of four experimental replicates.

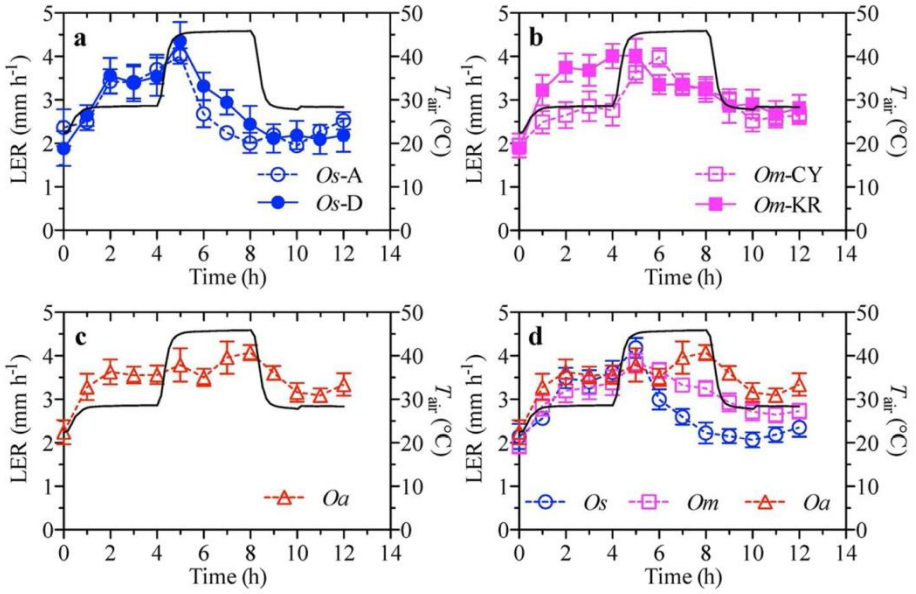

112x77mm (300 x 300 DPI)

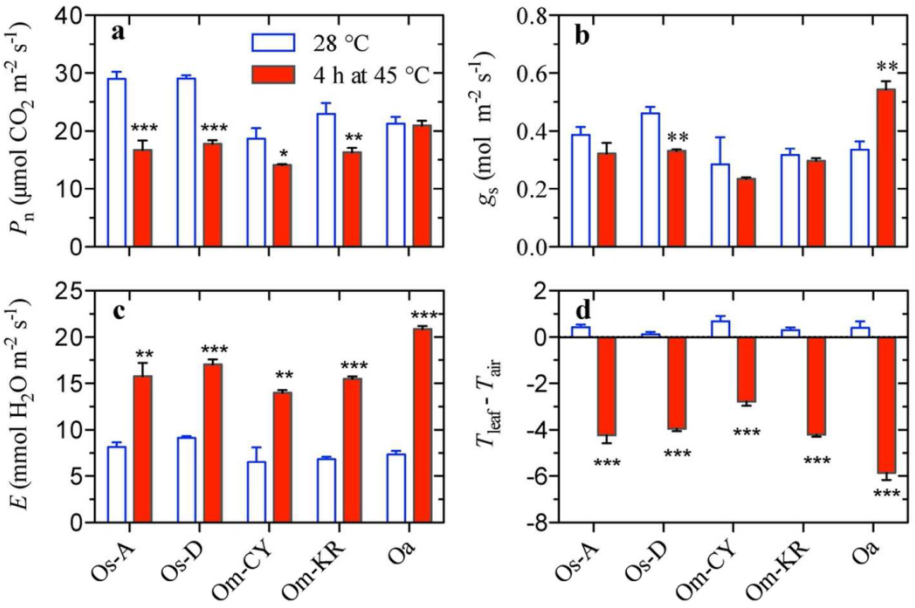

105x76mm (300 x 300 DPI)

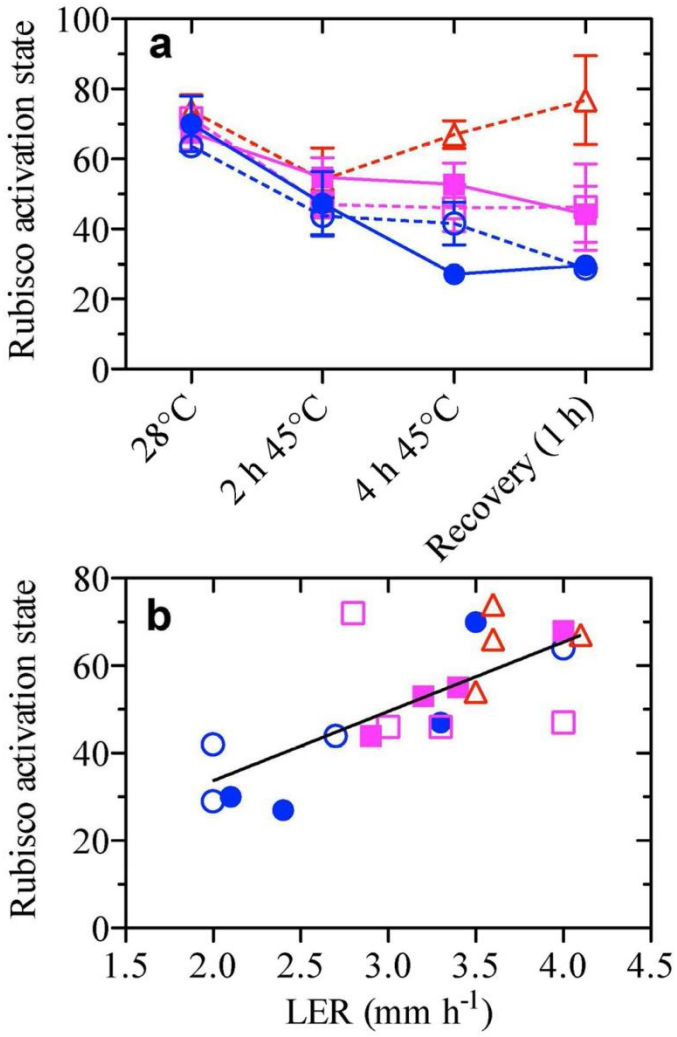

114x156mm (300 x 300 DPI)

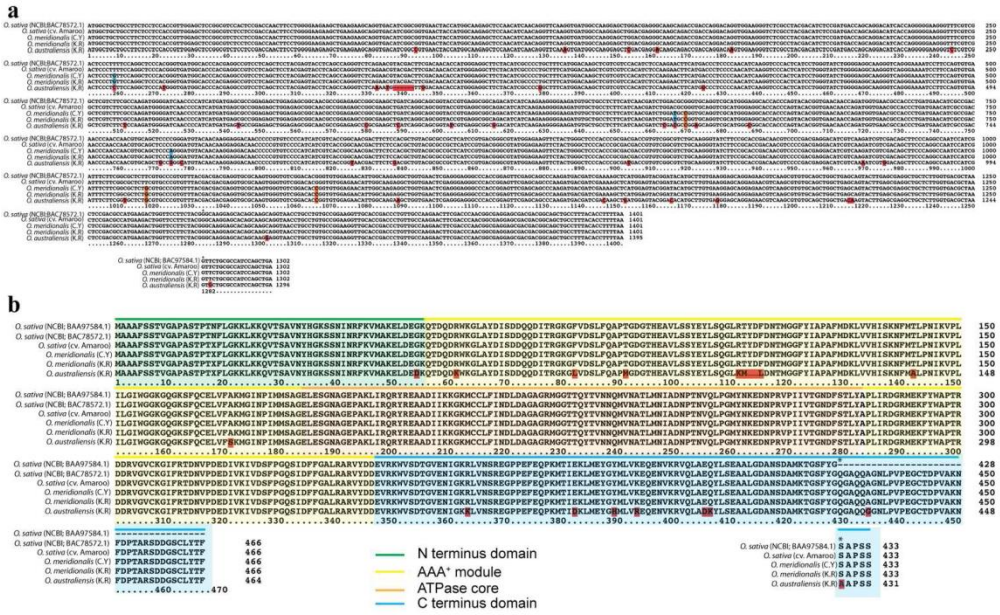

173x107mm (300 x 300 DPI)

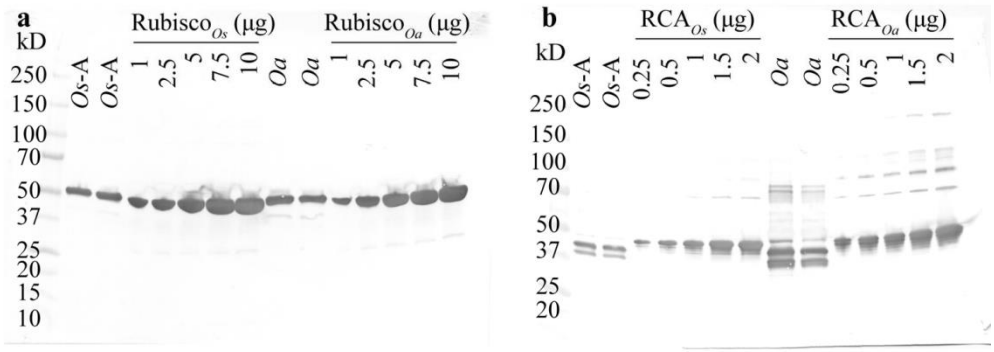

143x54mm (300 x 300 DPI)

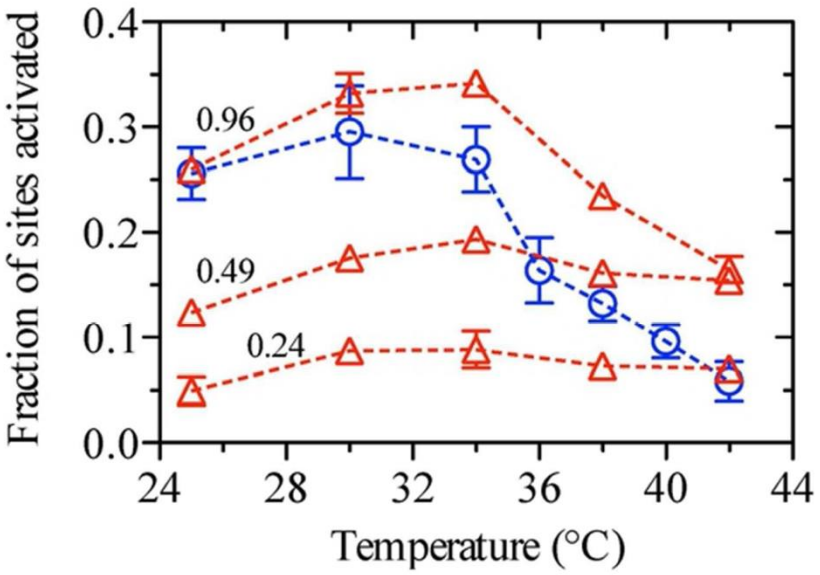

56x39mm (300 x 300 DPI)

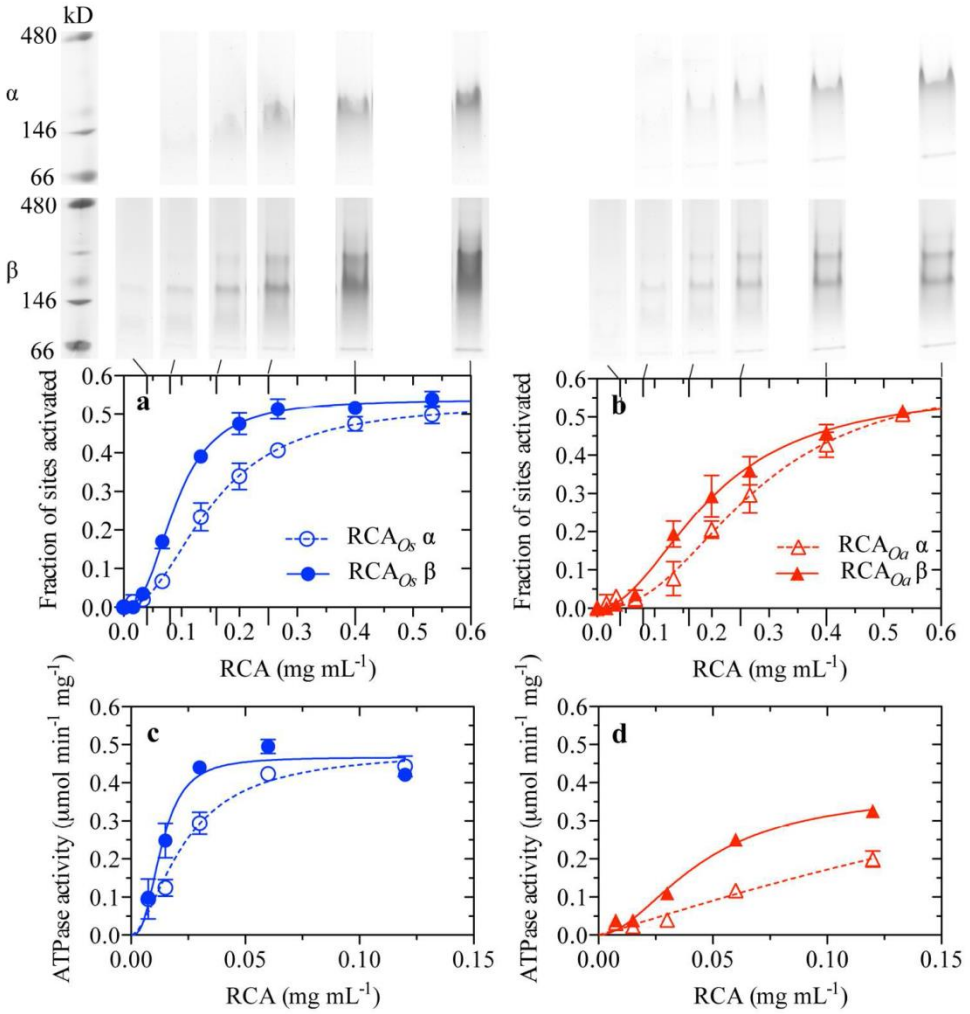

144x151mm (300 x 300 DPI)

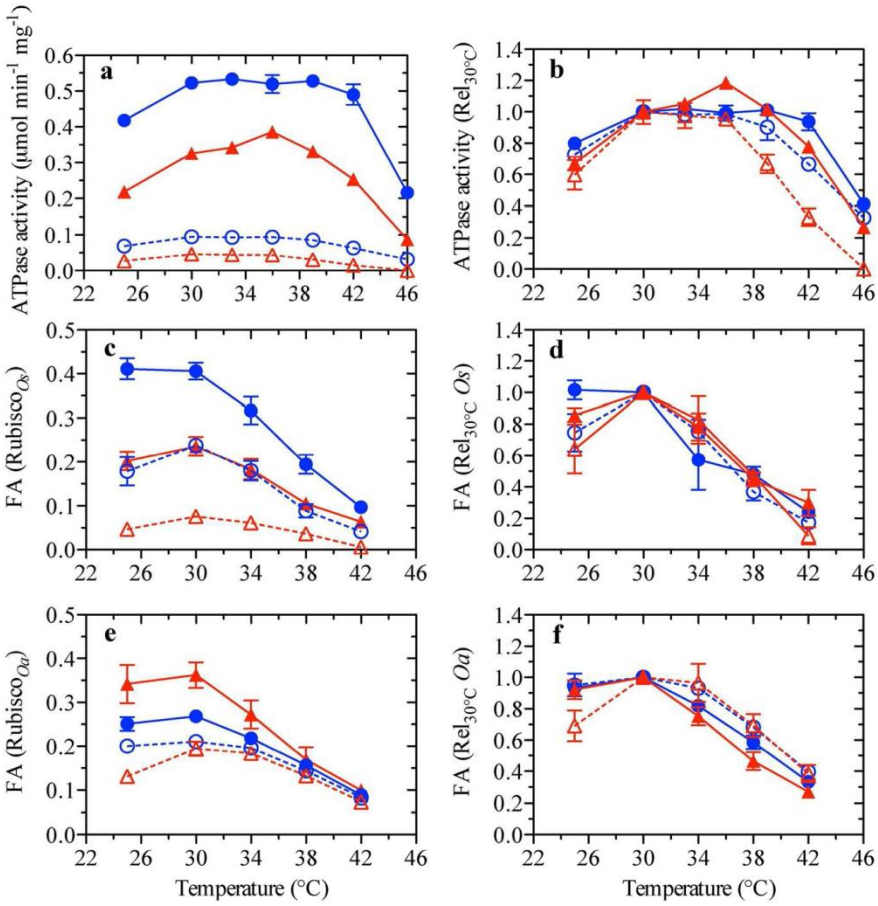

149x147mm (300 x 300 DPI)